

Effect of Temperature and Moisture on the Miscibility of Amorphous Dispersions of Felodipine and Poly(vinyl pyrrolidone)

PATRICK J. MARSAC,^{1,2} ALFRED C. F. RUMONDOR,¹ DAVID E. NIVENS,³ UMESH S. KESTUR,¹ LIA STANCIU,⁴ LYNNE S. TAYLOR¹

¹Department of Industrial and Physical Pharmacy, School of Pharmacy, Purdue University, West Lafayette, Indiana 47907

²Phase Definition and Materials Science, Merck & Co., Inc., West Point, Pennsylvania 19486

³Department of Food Science, Purdue University, 745 Agriculture Mall Drive, W. Lafayette, Indiana 47907

⁴School of Material Engineering, Purdue University, West Lafayette, Indiana 47907

Received 13 January 2009; revised 23 March 2009; accepted 9 April 2009

Published online 2 June 2009 in Wiley InterScience (www.interscience.wiley.com). DOI 10.1002/jps.21809

ABSTRACT: The physical stability of amorphous molecular level solid dispersions will be influenced by the miscibility of the components. The goal of this work was to understand the effects of temperature and relative humidity on the miscibility of a model amorphous solid dispersion. Infrared spectroscopy was used to evaluate drug–polymer hydrogen bonding interactions in amorphous solid dispersions of felodipine and poly(vinyl pyrrolidone) (PVP). Samples were analyzed under stressed conditions: high temperature and high relative humidity. The glass transition temperature (T_g) of select systems was studied using differential scanning calorimetry (DSC). Atomic force microscopy (AFM) and transmission electron microscopy (TEM) were used to further investigate moisture-induced changes in solid dispersions. Felodipine-PVP solid dispersions showed evidence of adhesive hydrogen bonding interactions at all compositions studied. The drug–polymer intermolecular interactions were weakened and/or less numerous on increasing the temperature, but persisted up to the melting temperature of the drug. Changes in the hydrogen bonding interactions were found to be reversible with changes in temperature. In contrast, the introduction of water into amorphous molecular level solid dispersions at room temperature irreversibly disrupted interactions between the drug and the polymer resulting in amorphous-amorphous phase separation followed by crystallization. DSC, AFM, and TEM results provided further evidence for the occurrence of moisture induced immiscibility. In conclusion, it appears that felodipine-PVP solid dispersions are susceptible to moisture-induced immiscibility when stored at a relative humidity $\geq 75\%$. In contrast, the solid dispersions remained miscible on heating. © 2009 Wiley-Liss, Inc. and the American Pharmacists Association *J Pharm Sci* 99:169–185, 2010

Keywords: amorphous; phase separation; poly(vinylpyrrolidone); water

INTRODUCTION

The utility of amorphous molecular level solid dispersions can only be realized if the influence of environmental stresses, particularly moisture sorption and temperature fluctuations, on physical

Correspondence to: Lynne S. Taylor (Telephone: +1-755-496-6614; Fax: +1-755-494-6545; E-mail: ltaylor@pharmacy.purdue.edu)

Journal of Pharmaceutical Sciences, Vol. 99, 169–185 (2010)
© 2009 Wiley-Liss, Inc. and the American Pharmacists Association

stability is well understood. Physical stability is a major concern because crystallization of the drug will negate the dissolution rate advantages conferred by using an amorphous system. Solid dispersions are exposed to various conditions of temperature and relative humidity (RH) during production and storage, and are subjected to stress conditions during accelerated stability testing. Residual water may remain postprocessing or water may be sorbed from the environment during storage. Water has been shown to increase the nucleation rate of drugs from amorphous molecular level solid dispersions.¹ It may act as an antiplasticizing agent at very low concentrations,² a plasticizing agent at higher concentrations,^{3,4} and may change the thermodynamic driving force for crystallization.⁵ It is well documented that the crystallization rate of pharmaceutical systems can be significantly influenced by the presence of a small amount of water.^{1,6,7} Furthermore, water may act as a competitor for hydrogen bonding sites within the polymer matrix. It is also relevant to consider the excursions in temperature that may be experienced by a solid dispersion. Temperature fluctuations may be experienced during manufacture (e.g. during melt extrusion), accelerated stability testing, and product storage and it is well known that increased temperature can decrease the stability of amorphous systems through dramatic influences on molecular mobility.⁸

Although the phenomenological effects of moisture and temperature on solid dispersions are well documented, the effect of these stresses on the miscibility and molecular level structure of amorphous solid dispersions has not been widely investigated. The stability of amorphous molecular level solid dispersions will be influenced by the miscibility of the components, which in turn is dictated by the thermodynamics of mixing. Since the entropy of mixing will always be favorable, the mixing enthalpy is the key factor which will influence miscibility. The enthalpic component of the mixing free energy is determined by the relative strength of the cohesive interactions (drug–drug and polymer–polymer interactions) and adhesive interactions (drug–polymer interactions). However, little work has been done to address how these interactions respond to environmental stresses such as fluctuations in relative humidity and temperature. The purpose of this work was to understand, on a molecular level, how the structure of solid dispersions is affected by temperature and relative humidity. To achieve this, infrared (IR)

spectroscopy was used to probe the impact of temperature and moisture on the molecular level structure of a model solid dispersion system comprised of the hydrophobic calcium channel blocker, felodipine, and the hydrophilic polymer, poly(vinyl pyrrolidone) (PVP). Several additional experimental techniques were also employed to better understand and confirm the phenomena observed using IR spectroscopy.

EXPERIMENTAL SECTION

Materials

Felodipine was a gift from AstraZeneca (Södertälje, Sweden). Poly(vinyl pyrrolidone) K29/32 was purchased from Sigma–Aldrich Co. (St. Louis, MO). Ethanol and dichloromethane were obtained from Aaper Alcohol and Chemical Co. (Shelbyville, KY) and Mallinckrodt Baker, Inc., (Paris, KY), respectively.

Methods

Preparation of Spin-Coated Films on Various Substrates

Spin-coating was performed using a KW-4A spin-coater (Chemat Technology, Inc., Northridge, CA) inside a glovebox at a relative humidity of less than 10%. For Fourier transform infrared (FTIR) spectroscopy studies, felodipine was combined with PVP K29/32 and the mixture was dissolved together in ethanol or 1:1 (w/w) mixture of ethanol and dichloromethane. All mixtures were visually inspected to confirm that the drug and the polymer were fully dissolved, and the systems formed uniform one-phase solutions. One to two drops of the solution were then placed on a clean, rotating ZnSe substrate (Specac, Incorporated, Woodstock, GA) and the spin-coated film was heated to 90–100°C for several minutes to remove remaining volatiles. The resulting optically transparent film was analyzed by FTIR.

To study the effects of the presence of moisture in the solvent on drug–polymer specific interactions, 0.1 mL water was added for every 1.9 mL solvent using a calibrated Fisherbrand[®] volumetric auto-pipetter (Fisher Scientific, Pittsburgh, PA). Following visual inspection that the drug and the polymer were fully dissolved, the solution was spin coated onto an infrared-substrate as described above, and the resulting films were heated to 90°C for up to a minute.

Atomic force microscopy (AFM) experiments were conducted using samples spin-coated onto precleaned glass microscope slides or cover slips, again followed by heating to 90°C to remove residual volatiles. Multiple samples were prepared from the solutions and stored in desiccators kept at 94% RH using a saturated solution of KNO₃. Samples were removed from the desiccator at different time points, and immediately dried under vacuum for at least 24 h prior to imaging experiments. Control samples were stored at 0% RH over phosphorus pentoxide.

Infra-Red Spectroscopy

Infrared spectra of the thin films were obtained in absorbance mode using a Bio-Rad FTS 6000 spectrophotometer (Bio-Rad Laboratories, Cambridge, MA) equipped with global infrared source, KBr beamsplitter, and DTGS detector. The scan range was set from 500 to 6000 cm⁻¹ with 4 cm⁻¹ resolution, and at least 64 scans were coadded. During measurements, the spectrometer was purged with conditioned air to prevent spectral interference from water vapor and CO₂.

Variable Temperature FTIR Spectroscopy

A Specac Variable Temperature Cell with a 4000 series controller (Specac, Incorporated) was mounted on the spectrometer. The ZnSe IR transparent substrates were placed in the temperature control cell using the variable temperature cell solids holder (Specac, Incorporated). After a background spectrum was collected at each temperature, the substrate was removed, thin films were prepared as described above, and the sample was again placed in the spectrometer for analysis at various temperatures and relative humidities. The location of the peaks associated with each type of hydrogen bond interaction was determined using a 21 point Savitzky-Golay second derivative using GRAMS/AI V.7.02 software (Thermal Fisher Scientific, Inc., Waltham, MA).

For the kinetic study of drug-polymer mixing, thin films of amorphous solid dispersion samples on ZnSe IR substrates that had been stored at 94% RH for 4 h were dried, placed in the variable temperature cell solids holder, and heated to 125°C. Periodically, spectra of the samples were collected.

Controlled Relative Humidity Storage Conditions

Materials were stored at various relative humidities using desiccators and saturated salt solutions of magnesium chloride (33% RH), potassium carbonate (43% RH), sodium bromide (58% RH), sodium chloride (75% RH), potassium chloride (84% RH), and potassium nitrate (94% RH).⁹ Samples quoted as 0% RH were stored over phosphorous pentoxide. Unless otherwise stated, samples were dried either under vacuum or by exposure to a stream of dry N₂ gas prior to analysis.

In addition, the thin films were analyzed under controlled humidity conditions using the Specac Variable Temperature Cell (Specac, Incorporated) coupled with a RH 200 relative humidity generator (VTI Corporation, Hialeah, FL). A pair of ZnSe windows (Specac, Incorporated) isolated the temperature control cell from the spectrometer.

Preparation of Bulk Amorphous Materials

Amorphous molecular level dispersions of the drug and polymer were prepared by solvent evaporation. PVP K29/32 was dried over phosphorous pentoxide for no less than 1 week, mixed with felodipine in a glove-box kept under 10% RH, and then the mixture was dissolved in 100% ethanol. The solvent was removed using a rotary evaporator apparatus (Brinkman Instruments, Westbury, NY). The samples were then placed under vacuum for at least 12 h prior to DSC measurements or vapor sorption experiments.

Dynamic Vapor Sorption

Water uptake of select amorphous molecular level solid dispersions of felodipine and PVP were measured using a symmetrical gravimetric analyzer (SGA-100; VTI Corporation) at 25°C. Bulk samples were prepared as described above, 10–15 mg of sample were loaded into the gravimetric analyzer, dried for 6 h at 40°C under nitrogen, and subsequently exposed to a relative humidity of 75%, 85%, and 95% for 5 h.

Differential Scanning Calorimetry

The glass transition temperature (T_g) was measured using a TA Q10 DSC equipped with a refrigerated cooling accessory (TA Instruments, New Castle, DE). Operating in standard mode, the instrument was calibrated for temperature using benzophenone (Sigma-Aldrich, Inc.) and indium (Perkin-Elmer Corporation, Norwalk, CT) and

the enthalpy response was calibrated using indium. Nitrogen, 45 mL/min, served as the purge gas and reference and sample pans were matched for weight to within 0.01 mg.

Samples of 4–6 mg were weighed into open DSC sample pans and then placed in desiccators at 0, 75, 84, and 94% RH for about 10 h. Samples were then removed from the desiccators and placed in a vacuum oven for 10–12 h, and then transferred to the DSC. Prior to scanning, the samples were exposed to an in situ nitrogen purge for 1–17 h.

Atomic Force Microscopy (AFM) and Transmission Electron Microscopy (TEM)

Atomic force microscopy (AFM) experiments were conducted on several samples using alternating current (AC) mode (analogous to Tapping ModeTM) using a closed-loop MFP-3D-BIO AFM system (Asylum Research, Santa Barbara, CA) and AC240 probes (Olympus). Each Si probe has a rectangular cantilever (approximately 240 μm length \times 30 μm width \times 2.7 μm thick and with a backside coating of Al) with an approximate spring constants of 2 N/m and a tip radius of less than 10 nm. The cantilevers were oscillated near resonance (70 kHz) by the system using a piezoelectric shake transducer. Both topographical and phase information were obtained from untreated films and samples that were exposed to 94% RH for various time intervals. Topographical images were generated using both piezo-voltage (voltage used to move piezoelectric actuators and referred to as height images) and the z-sensor signals. The z-sensor (z-LDVT) is used to correct for nonlinearity inherent in the piezo-voltage data, thereby producing more accurate measurement of heights. Phase images were generated by measuring phase shifts that are caused by interactions between the probe-tip and sample. Phase shifts are obtained by determining the phase angle between the oscillating cantilevers (optical lever signal) relative to the drive signal. The phase shift is tuned to 90° at the beginning of each experiment by oscillating the cantilever above the sample and away from the influence of any surface interactions. Phase images are used routinely in AFM to identify regions that have different mechanical and/or chemical properties within a single image. Images were subjected to a zero-ordered plane-fitting function as necessary, while untreated felodipine-PVP films required an additional zero-ordered flattening function, which is used to align the scan-lines of these extremely flat images.

Electron diffraction and TEM experiments were conducted on a FEI/Philips CM-10 Bio-Twin TEM instrument (FEI Company, Hillsboro, OR) operating at 80 kV. Samples were prepared by spin-coating onto 200 mesh carbon coated Copper TEM grids (SPI supplies, West Chester, PA), followed by heating to 90°C to remove residual volatiles. Freshly prepared samples of the solid dispersions (30% PVP-Felodipine) were stored in desiccators kept at 94% RH using a saturated solution of KNO_3 . Samples were removed at predetermined time intervals from the desiccators and immediately dried under vacuum overnight prior to imaging experiments. Control samples were stored at 0% RH over phosphorus pentoxide. Electron diffraction was used to confirm the presence or absence of crystallinity in the samples. Hole-like features were seen in the micrographs and were attributed to solvent evaporating from the grids on spin coating. Images shown are representative of the general trends observed in the samples.

RESULTS

Variable Temperature FTIR

Figure 1 shows the effect of temperature on the NH-stretching region of felodipine and amorphous molecular level solid dispersions of felodipine with 0, 30, 37, 46, and 74 wt% PVP. The NH region reflects the participation of felodipine in both cohesive and adhesive hydrogen bonding interactions and has been described in detail previously.¹⁰ Briefly, at 25°C, drug–drug hydrogen bonding yields a NH peak centered at 3341 cm^{-1} while drug–polymer hydrogen bonding results in a NH peak at 3290 cm^{-1} , and no significant spectral interference from PVP is seen in this region. On heating, the peak in pure amorphous felodipine associated with the drug hydrogen bonding with other drug molecules shows a shift in position from 3337 cm^{-1} at 5°C to 3350 cm^{-1} at 160°C (Fig. 2a), indicating weakening of cohesive hydrogen bonding with temperature in agreement with previous results.¹¹ The solid dispersion containing 30 wt% PVP shows a shift in the peak associated with the hydrogen bonding between the drug and the polymer from 3288 cm^{-1} at 5°C to 3296 cm^{-1} at 160°C. There is a corresponding increase in peak position for the drug–drug interactions. In solid dispersions with a high concentration of PVP, the peak arising from the adhesive interactions becomes more dominant

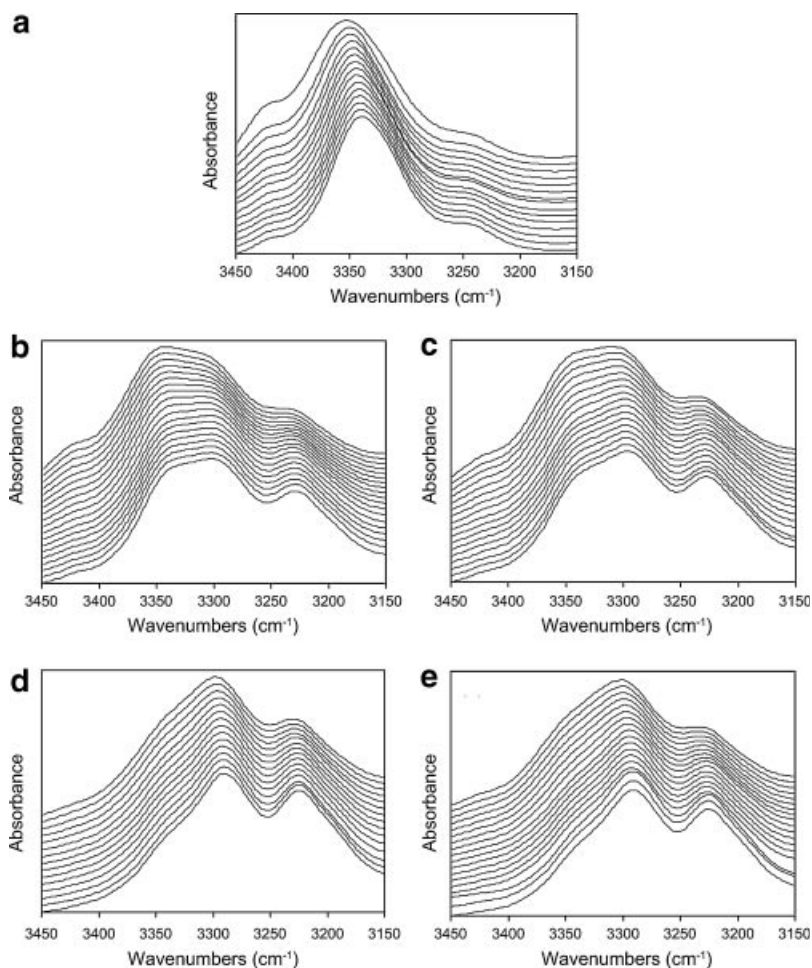


Figure 1. Amorphous molecular level solid dispersions of felodipine with (a) 0, (b) 30, (c) 37, (d) 46, and (e) 74 wt% PVP as a function of increasing temperature; 0°C (bottom spectrum) to as high as 180°C (top spectrum). Temperature intervals between spectra are 5–15°C.

in the spectrum relative to the drug–drug peak which appears as a shoulder. It can be clearly seen from the spectra shown in Figure 1, that drug–polymer hydrogen bonding interactions persist up to the melting point of the drug.

Figure 2 gives a more detailed perspective of how the peak positions vary with temperature for pure amorphous felodipine relative to a solid dispersion containing 30 and 54 wt% PVP. The increase in peak positions with temperature are indicative of a gradual weakening of intermolecular hydrogen bonding.^{11–17} It is interesting to note that a change in slope of peak position versus temperature occurs close to the glass transition temperature of each system. For instance, consider the amorphous molecular level solid dispersion containing 30 wt% PVP. The glass transition temperature as measured by DSC is 57°C ($\pm 5^\circ\text{C}$).

The slopes associated with both the drug–drug and the drug–polymer interactions show a clear discontinuity at about 60°C. Similarly, the dispersion containing 54 wt% PVP has a glass transition temperature of 89°C ($\pm 5^\circ\text{C}$) as measured by DSC whereas a change in slope in the peak position is observed at a similar temperature ($\sim 90^\circ\text{C}$). This observation has been made previously for amorphous felodipine alone,¹¹ and it appears that both the adhesive and cohesive interactions in solid dispersions also weaken as the glass transition temperature is exceeded. Interestingly, no hysteresis is seen in the spectra on heating followed by cooling. This is clearly shown by Figure 3 where it can be seen that the peak positions for adhesive and cohesive interactions superimpose during a heating and a cooling run. This is an important result since it shows that

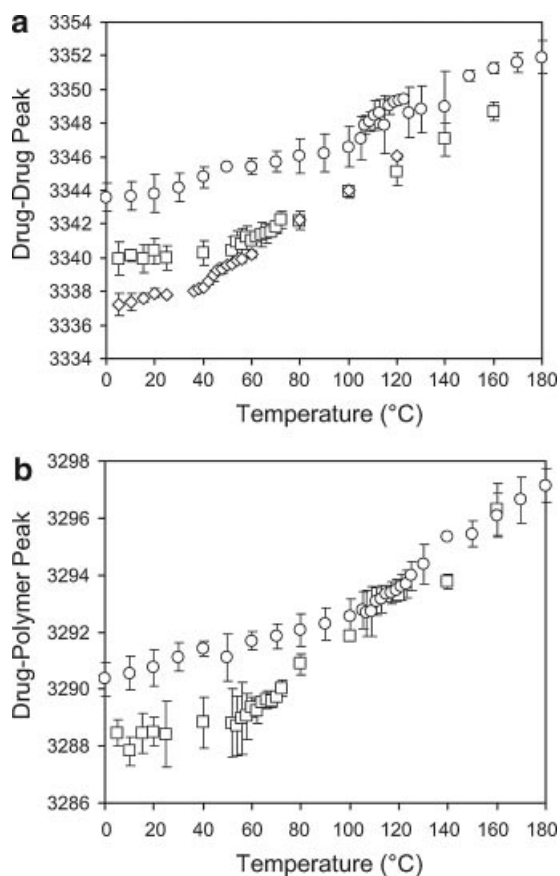


Figure 2. Peak position of NH stretch attributed to drug–drug hydrogen bonding interaction (a) and drug–polymer hydrogen bonding interaction (b) for amorphous molecular level solid dispersions of felodipine with 0 wt% PVP (\diamond), 30 wt% PVP (\square), and 54 wt% PVP (\circ). Error bars represent average of three trials.

the effects of heating on the intermolecular interactions are reversible. Furthermore, this observation confirms that the system is in “equilibrium” from the perspective of maximizing adhesive and cohesive interactions, during the variable temperature experiments.

Variable Relative Humidity FTIR

Figure 4 shows amorphous molecular level solid dispersions of felodipine with 30 wt% PVP exposed to 33, 58, and 75% RH for 1 week. These spectra were taken in a humidity controlled environment as described above which largely eliminated the background interference from water vapor. From these data, the increased water uptake with increasing relative humidity can be clearly seen from the appearance of a broad peak at higher

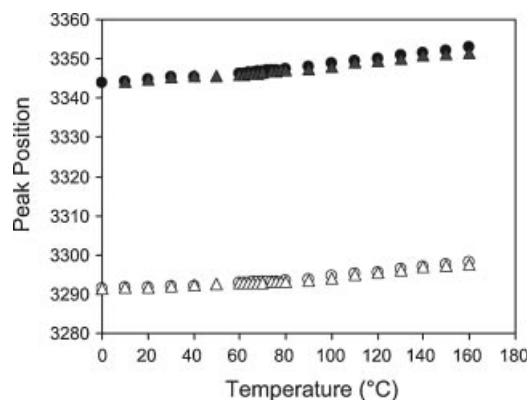


Figure 3. Peak position associated with drug–drug hydrogen bond interactions (closed symbols) and drug–polymer hydrogen bond interactions (open symbols) for amorphous molecular level solid dispersions of felodipine with 37 wt% PVP as a function of increasing temperature (\blacktriangle) and decreasing temperature (\bullet).

wavenumbers associated with the OH stretch of water. However, of greater significance are the differences observed in the NH stretching region whereby the peaks associated with drug–polymer interactions decrease in intensity relative to the peaks associated with the drug–drug interactions. The changes in the spectra are small following storage at 33 and 58% RH but are quite distinct for the systems exposed to 75% RH. However, because of the influence of the overlapping water band which obscures this region to some degree, spectra were also obtained following exposure to water and drying. Figure 5 shows the same systems shown in Figure 4 after drying over phosphorous pentoxide for 1 week. The changes in the hydrogen bonding patterns seen in the presence of moisture persist.

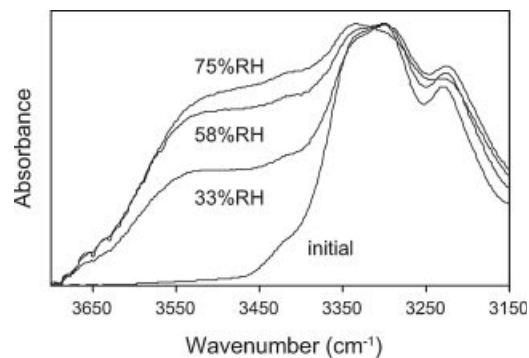


Figure 4. NH stretching region of amorphous molecular level solid dispersions of 69.7 wt% felodipine and 30.3 wt% PVP after exposure to 33, 58, and 75% RH for 1 week, 25°C.

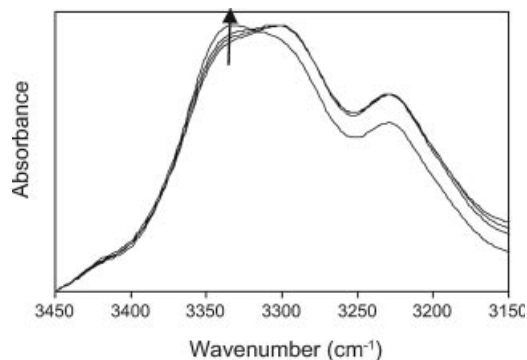


Figure 5. NH stretching region of amorphous molecular level solid dispersions of 69.7 wt% felodipine with 30.3 wt% PVP after exposure to 0, 33, 58, and 75% RH, 25°C for 1 week (ordered as indicated by arrow) followed by drying in a desiccator at 0% RH for 1 week to remove the water. The changes observed in the NH region as a result of water uptake persist in the spectra of the dried materials.

At even higher relative humidity, the dispersions studied here begin to take up increasingly large amounts of water. For instance, as shown in Figure 6, it becomes clear that the dispersion containing 70 wt% PVP shows an upturn in water content as the relative humidity increases beyond about 75%. This result was observed to be consistent with all of the solid dispersions studied here and selected results are shown in Table 1. The consequences of increased water activity in the solid dispersion become clear when examining Figure 7 which shows the effect of increased relative humidity for several felodipine-PVP amorphous molecular level solid dispersions exposed to high relative humidity and subsequently dried. For both the solid dispersion containing 30.3 wt% PVP and the solid dispersion

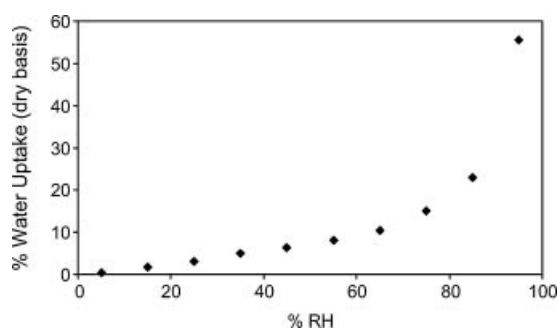


Figure 6. Water vapor sorption as a function of relative humidity for a solid dispersion containing 70 wt% PVP. As the relative humidity approaches and exceeds 75%, the water uptake drastically increases.

Table 1. Weight Percentage Water Uptake Based on the Initial Mass of the Solid Dispersion for Dispersions Containing 30, 50, and 70 wt% PVP Stored at 75, 85, and 95% RH and Equilibrated for 5 h

wt% PVP	% Relative Humidity		
	75	85	95
30	5.6 (0.1)	7.6 (0.1)	24.6 (1.1)
50	4.8 (0.2)	9.9 (0.1)	40.3 (0.1)
70	15.0 (1.2)	23.3 (1.8)	55.5 (5.7)

Numbers in parenthesis represent range of duplicate measurements.

containing 46.5 wt% PVP, clear changes in the hydrogen bonding patterns are observed and these are more exaggerated than for the systems shown in Figure 5. Also shown in Figure 7 are the crystalline and amorphous spectra of felodipine. Following exposure to high RH, the spectra of the dried dispersions increasingly resemble the spectrum of pure amorphous felodipine. It is clear that the spectral changes cannot be accounted for by any significant degree of crystallization of the drug. These results suggest that the number of drug-polymer interactions have been irreversibly compromised following exposure to moisture with increasingly dramatic effects being seen at 75% RH and above. The increased extent of drug-drug hydrogen bonding compared to drug-polymer hydrogen bonding strongly suggest that the systems are undergoing amorphous-amorphous phase separation to a drug-rich amorphous phase and a polymer-rich amorphous phase. These spectroscopic changes could be observed for samples exposed to high RH conditions for short periods of time (2–24 h); when stored for longer periods of time, spectral changes indicated that crystallization had occurred. Crystallization was confirmed using polarized light microscopy.

Impact of Moisture in Solvent During Sample Preparation

Figure 8 shows the NH stretching region of felodipine-PVP amorphous solid dispersion samples containing 30% and 50% (w/w) PVP prepared using a solvent evaporation technique whereby water was added to the solvent. During spin-coating onto the substrate, it was expected that the more volatile components of the solvent (ethanol and dichloromethane) would preferentially evaporate, leading to concentration of water.

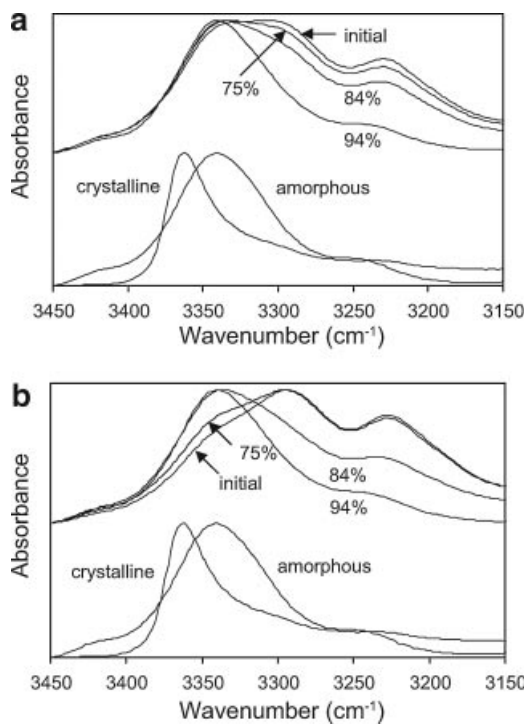


Figure 7. Amorphous molecular level solid dispersions of felodipine and 30.3 wt% PVP (a) and 46.4 wt% PVP (b) immediately after sample preparation and after storage at 75, 84, and 94% RH for 1 day. Also shown for comparison are the amorphous and crystalline spectra of felodipine. PVP does not exhibit any significant absorption in this region.

It is clear from Figure 8 that the intensity of the peak centered at 3290 cm^{-1} was reduced relative to the peak centered at 3345 cm^{-1} when water was present in the solution during spin-coating

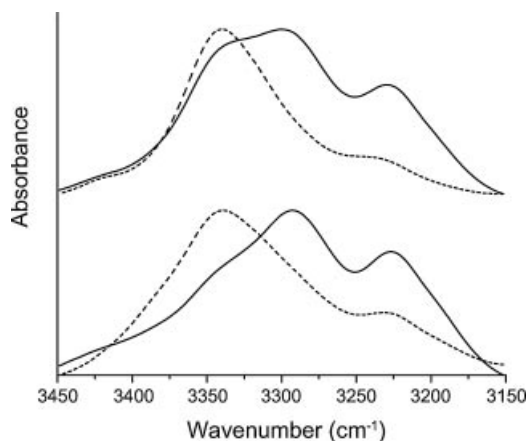


Figure 8. FT-IR spectra of amorphous dispersions of felodipine and 30 wt% (a) and 50 wt% (b) PVP prepared with water added to the solvent during production (dashed lines) and without water added (solid lines).

suggesting that the presence of water disrupted the potential for drug–polymer hydrogen bonds to be formed. The spectra of the samples prepared from a solvent-containing water strongly resemble those of solid dispersions samples (prepared from a dry solvent) after exposure to elevated RH. Thus it is apparent that the drug–polymer hydrogen bonds can be disrupted either by exposure to atmospheric moisture or by the presence of liquid water.

DSC Analysis

The DSC thermograms of the amorphous dispersions of felodipine with 46.5 wt% PVP are shown in Figure 9. Although several thermal events are observed, all of the samples appear to show a glass transition-like event at about $45\text{--}50^\circ\text{C}$, which is close to that reported for pure felodipine.^{18,19} This suggests the presence of a drug–rich amorphous phase. For comparison, the expected T_g for a dispersion containing 46.5 wt% PVP is around 80°C .¹⁹ Figure 9d, which was the most rigorously dried sample, also displays a thermal event with an onset at $\sim 124^\circ\text{C}$. This may represent a second glass transition event. Since pure PVP K29/32 has a glass transition temperature of about 150°C ,^{20,21} it is likely that this potential second glass transition is associated with a phase that contains either (1) a significant amount of drug initially or (2) drug which has remixed with the polymer during the experiment. A second explanation for the event occurring at $\sim 124^\circ\text{C}$ is that it may be the result of the depressed melting point of felodipine in the presence of PVP although no recrystallization exotherm was observed. Clearly, the non-isothermal nature of the DSC measurement makes interpretation of the high temperature events difficult. Second scans are also shown in Figure 9 and it appears that the sample remixes after heating; all samples give a single glass transition temperature at around 80°C which is similar to the expected value for a dispersion containing 46.5 wt% PVP.

The process of remixing was explored further as shown in Figure 10. A dispersion of the same concentration, 46.5 wt% PVP was stored at 94% RH for 1 day, dried under N_2 in the DSC for 15 h, and cycled through increasing maximum temperatures. The first scan reveals a strong enthalpic recovery which is largely absent in subsequent scans. However, most notable from this data is the shift in the thermal event to an increasingly high

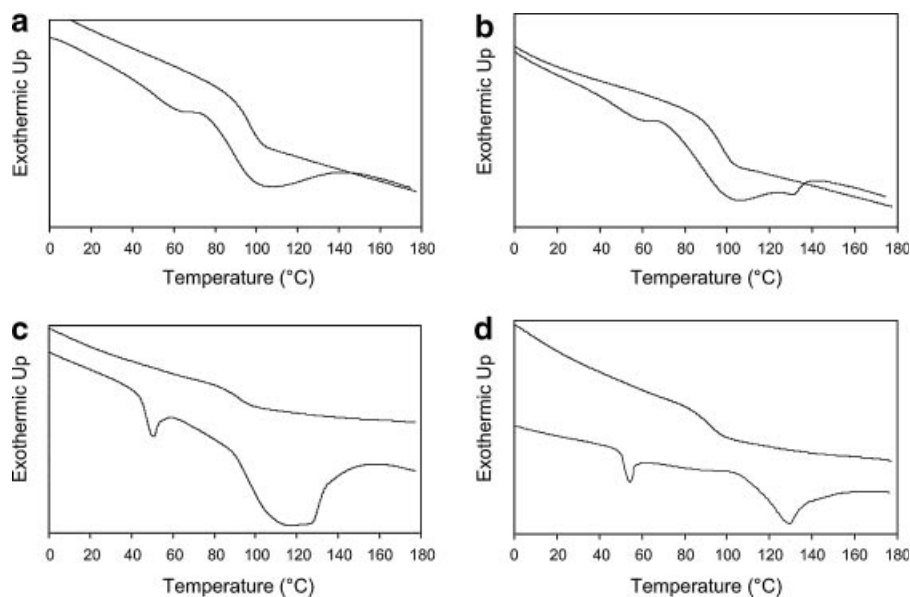


Figure 9. DSC thermograms of amorphous molecular level solid dispersions of felodipine with 46.5 wt% PVP. Samples were stored at 75% RH (a), 84% RH (b), and 94% RH (c and d) for about 12 h. Samples (a–c) were dried under vacuum overnight and subsequently purged with nitrogen for 1 h prior to running the experiment. Sample (d) was put through the same drying procedure and in addition was dried in the DSC for 17 h prior to running the scan (see text).

temperature with each sample cycle likely reflecting the remixing of the initially phase separated system. During the last scan, an exothermic event is observed followed by an endothermic event, probably indicating the sample has crystallized and melted. As described previously, the non-isothermal nature of DSC may not provide an accurate description of the sample at any given

temperature and is further complicated by the kinetics of the measurement as compared to the timescale of the event being measured. Therefore, additional evidence for remixing at high temperature was sought using FTIR spectroscopy.

Kinetic IR Spectroscopy of Phase Separated Systems at 125°C

Figure 11 shows the NH stretching region of the infrared spectrum of a felodipine-PVP amorphous solid dispersion sample containing 50% (w/w) PVP following storage at 94% RH and subsequent drying. It can be seen from Figure 11 that, when held at 125°C, the peak centered at 3290 cm^{-1} increased in intensity relative to the peak centered at 3345 cm^{-1} , indicating that drug-polymer hydrogen bonding interactions were being formed as a result of remixing of the drug and the polymer.

To further assess changes in the extent of drug-polymer interactions during heating, the ratio of the relative intensity of the peak centered at 3290 cm^{-1} to the peak centered at 3345 cm^{-1} was determined and plotted against the natural logarithm of time as shown in Figure 12. The results show that as heating progressed, the ratio

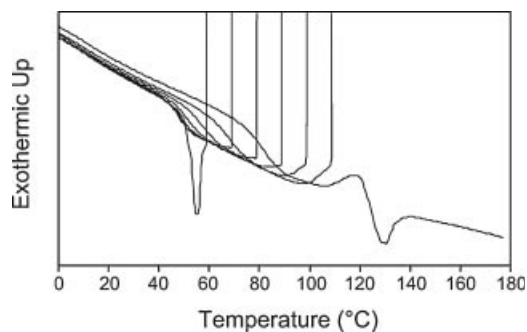


Figure 10. DSC thermogram of amorphous molecular level solid dispersion of felodipine with 46.5 wt% PVP. Sample was stored at 94%RH for 1 day, dried under nitrogen in the DSC for 15 h and cycled up to an increasingly high temperature. The maximum temperature of subsequent cycles was 60, 70, 80, 90, 100, and 110°C, respectively, followed by heating up to 175°C.

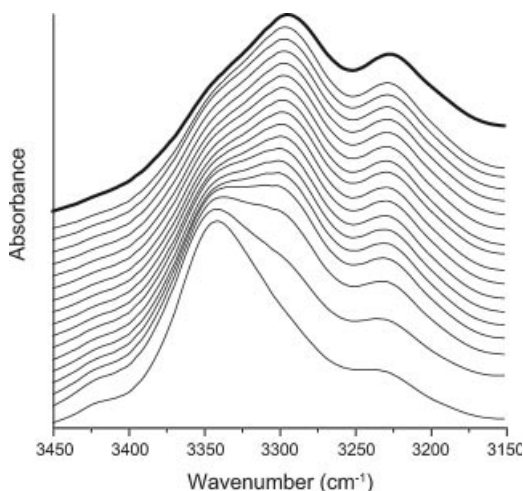


Figure 11. FT-IR spectra of NH stretching region of amorphous solid dispersion of felodipine with 50% PVP. The sample was stored at 94% RH for approximately 4 h, then dried using a dry air purge for an hour. Subsequently, the sample was heated to 125°C, and the infrared spectra collected; they are (bottom to top): initial, and after 5, 10, 15, 20, 25, 30, 45, 60, 90, 120, 150, 240, 300, 360, 420, and 1500 min. The top-most spectrum (thicker line) shows a solid dispersion sample at the same drug-to-polymer ratio that was never exposed to moisture.

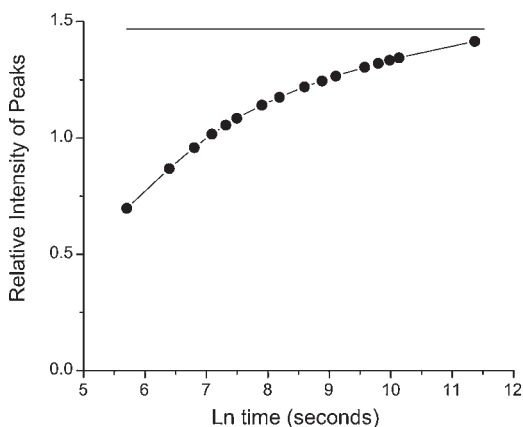


Figure 12. Relative height of IR peak centered at 3290 cm^{-1} (assigned to the NH stretching of drug moiety when hydrogen bonded to the carbonyl moiety of PVP) to the peak centered at 3345 cm^{-1} (assigned to the NH stretching of drug moiety when hydrogen bonded to the carbonyl moiety of other drug molecules) plotted as a function of ln time (in seconds) following heating at 125°C. The horizontal line at the top represents the relative height of these peaks calculated from the spectrum of a solid dispersion sample that was never exposed to moisture.

of the peak intensities approached that of the equivalent solid dispersion that had never been exposed to moisture. Extrapolation of the data indicates that the maximum level of drug-polymer hydrogen bonding will be reached after approximately 39 h.

Atomic Force Microscopy (AFM) and Transmission Electron Microscopy (TEM)

To verify the presence of different amorphous phases in felodipine-PVP solid dispersion systems following exposure to moisture at high relative humidity, AFM experiments were performed on samples containing 50% (w/w) PVP. The results of representative $5\ \mu\text{m} \times 5\ \mu\text{m}$ regions of interest, obtained as both topographical and phase maps, are presented in Figure 13. For each sample, imaging was performed on at least two to three different locations, and the results presented are representative of the general trends observed.

In general, AFM imaging showed that the drug-polymer films spin-coated onto microscope slides were smooth and featureless, as shown in the AFM topographical images (Fig. 13a). For example, the topographical root-mean-square (RMS) value for this surface was calculated as 0.22 nm. The AFM phase image (Fig. 13b) showed well mixed phases with no distinct regions, with an overall range of less than 5° .

When exposed to a humid environment, the felodipine-PVP film became cloudy when viewed by the naked eye and the AFM topographical images of these samples shows the development of features that increased the surface roughness of the sample. After 1-h storage at 94% RH, Figure 13c (note 100-fold z -scale change) shows the formation of features ranging from 11 to 20 nm in height, thereby increasing the surface RMS value to 17 nm. The corresponding phase image (Fig. 13d) shows development of distinct regions with phases differing by more than 50° , indicating that the feature may have different chemical and/or mechanical properties. After 2-h storage at 94% RH, topographical development in felodipine-PVP film continued (Fig. 13e), with height variations ranging from 15 to 34 nm (surface RMS value of 18 nm). After 4-h storage at 94% RH, shapes with distinct phase differences developed (Fig. 13g and h). Microscopic analysis under cross-polarized light of this sample showed regions with birefringence, indicating the presence of crystals (results not shown). The height of the distinct features

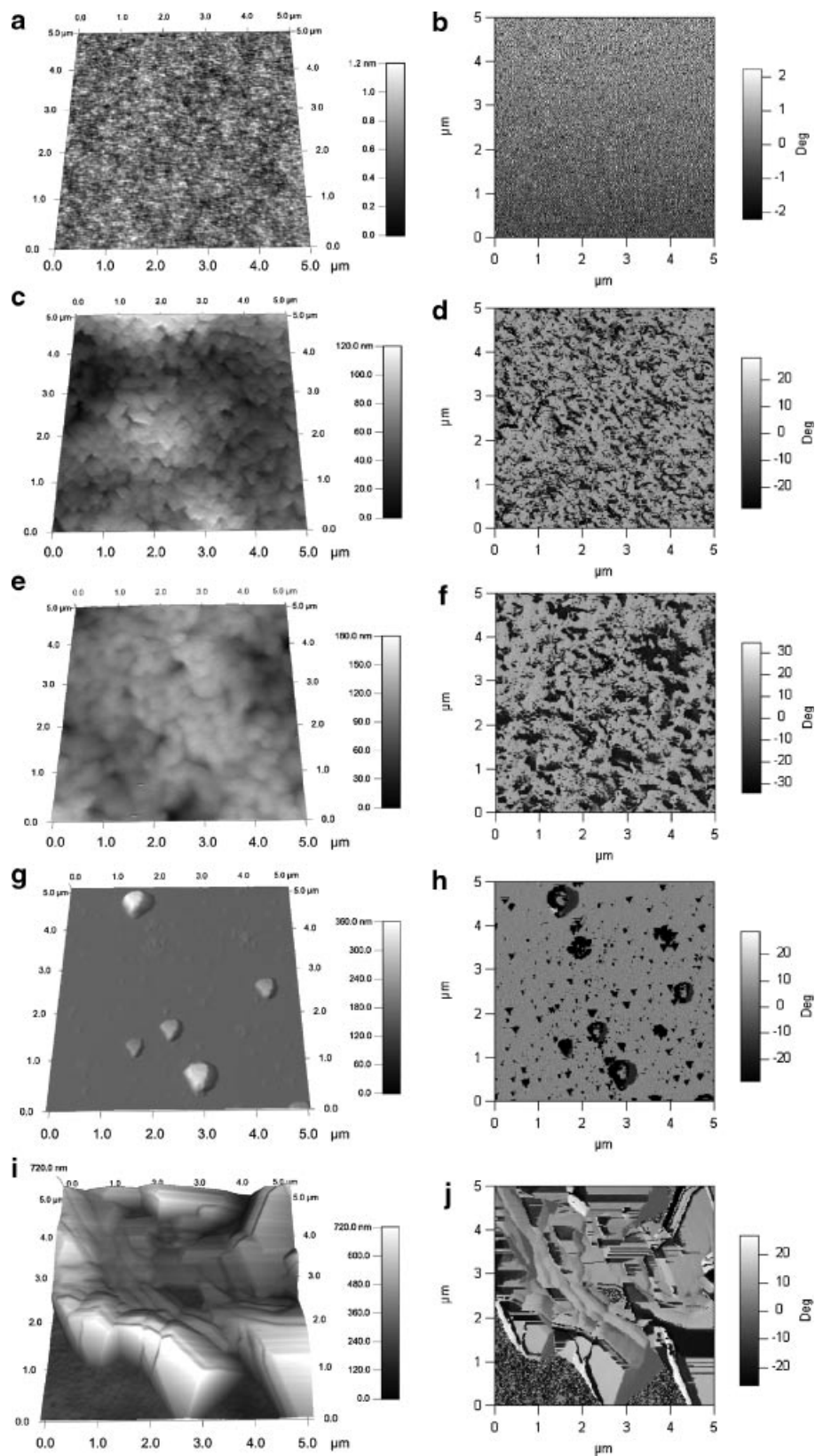


Figure 13. AFM topographical (left) and the corresponding phase (right) maps of different felodipine-PVP solid dispersion films containing 50% PVP (w/w) immediately after preparation (a and b), after 1-h (c and d), 2-h (e and f), 4-h (g and h), and 16-h (i and j) storage at 94% RH. The z-scales were adjusted to best show the results and image processing were applied when necessary (see text for details).

varied from 40 to 140 nm. The surface RMS value (minus these features) was 16 nm. After 16-h storage at 94% RH, large shapes with heights of 220–440 nm were present, which were presumably indicative of surface drug crystallization (Fig. 13i and j). Thus it appears that the system first undergoes amorphous-amorphous phase separation followed by crystallization of the drug rich regions. It should be noted that crystallization was not detected at exactly the same time point in similar samples using IR spectroscopy (e.g., Fig. 7), most likely because of the stochastic nature of nucleation, slight differences in sample preparation, and the different sensitivities of each technique to surface and bulk crystallization.

Figure 14a and b shows TEM photomicrographs of pure amorphous felodipine and PVP. The pure samples do not show any distinct features. The TEM image obtained from a solid dispersion containing 30% PVP-Felodipine (Fig. 14c) stored at 0% RH appeared to be well mixed, uniform and showed no distinct regions. In contrast, the solid dispersion exposed to 94% RH (Fig. 14d) appeared to show two distinct regions. No diffraction rings were observed for the sample shown in Figure 14d (see insert). Based on the absence of diffraction rings and presence of two distinct phases in the micrographs for the sample shown in Figure 14d, the sample appears to have undergone amorphous-amorphous phase separa-

tion. Following a longer storage period at 94% RH, samples were observed to have diffraction rings indicating that they had crystallized (data not shown).

DISCUSSION

Although it is well known that environmental stresses influence the crystallization tendency of drugs from amorphous molecular level solid dispersions, the mechanisms underlying the observed changes in crystallization rate are not well understood. Several recent studies have shown that crystallization tendency cannot be adequately predicted simply by considering changes in properties such as average relaxation times and T_g .^{5,10,20} In most general terms, crystallization from amorphous molecular level solid dispersions requires (i) the grouping of a critical mass of drug molecules and (ii) the orientation and alignment of these molecules to form a crystal lattice. Crystallization from highly viscous single component amorphous solids is kinetically rather than thermodynamically hindered.^{22–24} For amorphous solid dispersions, the presence of the polymer may reduce the thermodynamic driving force for crystallization by decreasing the chemical potential of the drug.^{25,26}

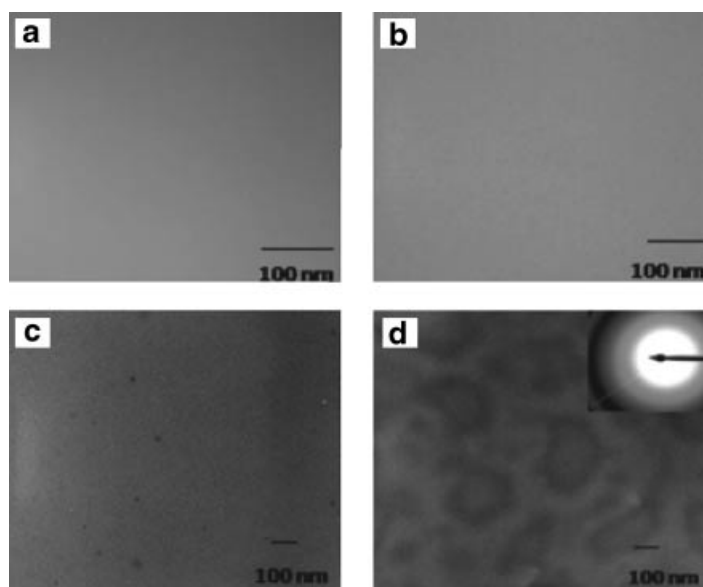


Figure 14. Transmission electron photomicrographs of (a) amorphous felodipine (b) PVP (c) 30% PVP-Felodipine exposed to 0% RH (d) 30% PVP-Felodipine exposed to 94% RH; the inset shows the diffraction pattern which indicates that the sample is amorphous.

In addition, the polymer appears to increase the kinetic barrier to crystallization.^{19,25} It has also been suggested that the polymer may act to impede transport of drug molecules to the crystalline phase.^{10,27,28} Regardless of the mechanism of crystallization, it is clear that the polymer has to be intimately associated with the drug molecules in order to be an effective inhibitor (i.e., the binary system must be miscible). Numerous studies have provided direct evidence for intermolecular interactions between drug and polymer in solid dispersions, confirming the ability of some systems to mix on a molecular level.^{10,29–31} However, because miscibility is both temperature and composition dependent, it is critical to assess how miscibility is affected by these key stressors.

Influence of Temperature

It is well known that changes of temperature can influence the miscibility of binary solutions, polymer blends and polymer solutions. For instance, phenol mixed with water shows an upper critical solution temperature of 66.8°C.³² In other words, one phase exists at temperatures above 66.8°C while two phases exist at temperatures below 66.8°C. In contrast, polystyrene mixed with cyclohexane³³ and nicotine mixed with water³⁴ exhibit both an upper critical solution temperature and a lower critical solution temperature. Thus there is a region of immiscibility over a certain temperature/composition range, and exceeding the lower critical solution temperature will lead to immiscibility. Hence from a theoretical perspective, amorphous solid dispersions composed of a drug and polymer might undergo mixing or demixing as a function of temperature if there a thermodynamic driving force and the kinetics of the process are not prohibitively slow.

Based on previous FTIR studies, it has been found that all compositions of felodipine-PVP solid dispersions prepared using a solvent evaporation technique are miscible at room temperature, showing clear evidence of intermolecular interactions between the drug and polymer.^{10,19,25} The variable temperature infrared spectroscopy results presented in Figure 1 clearly demonstrate that miscibility is maintained up to the melting point of the drug, as evidenced by the persistence of the drug–polymer hydrogen bond interactions. Although spectral changes are observed with temperature, these can be readily accounted for

by thermal expansion of the system.^{11,13–15,35} Indeed, the reversibility of the drug–polymer interactions as a function of temperature shown in Figure 8 is quite remarkable and indicates that the system is well mixed at all temperatures explored here. Thus, neither an upper nor a lower critical “solution” temperature was observed using spectroscopic interrogation of the systems, over the timescales of the experiments and the range of temperatures investigated, suggesting that this is a region of miscibility. Finally, it is noted that these observations are in good agreement with previous results where this two component system is predicted to be miscible based on T_g measurements and modeling of the mixing thermodynamics.²⁵

Influence of Absorbed Moisture

In addition to the well known effects of temperature on miscibility, the effects of composition changes have also been explored. For example, Lu and Zograf³⁶ found that the miscibility of indomethacin and citric acid was promoted by the addition of PVP. It has also been observed that different solvents can reduce mixing in polymer blends.^{37,38} Such solvent-induced phase separation has also been called the $\Delta\chi$ effect,^{39,40} and has a thermodynamic origin. Essentially, when the interaction parameters between the solvent and each of the two miscible components are very different, the solvent induces immiscibility. In another related example, a system consisting of a macromolecular dendrimer and benzene, it was observed that the miscibility of the system was very dependent on the water content, with small levels of moisture resulting in the formation of two liquid phases.⁴¹ There is also some evidence that moisture may promote phase separation in amorphous pharmaceutical systems.^{31,42} Given the propensity of amorphous solid dispersions to absorb moisture (Fig. 6), it is important to evaluate the influence of water on miscibility. Exposure to water vapor was found to promote immiscibility—both during preparation and during storage. Although the observed amorphous–amorphous immiscibility was challenging to characterize experimentally in the presence of the absorbed moisture, combining the results of the several experimental techniques employed made it possible to extract information about the extent of the phase separation. The FTIR results shown in Figure 7 suggest that the

amorphous-amorphous phase separation into drug-rich and polymer rich regions is far from complete at either 75% or 84% RH (4.8 and 9.9 wt% water, respectively as shown in Table 1). In particular, drug-polymer interactions still persist compared to the dispersion prior to moisture exposure (although at a reduced level). In contrast, following exposure to 94% RH (40.3 wt% water as shown in Table 1), the NH peak of the drug in the phase separated dispersion closely resembles that found in the pure amorphous drug, suggesting that the drug rich phase contains little polymer. Correspondingly, the polymer rich phase must be drug poor. This supposition is supported by the DSC results which show two T_g events, where the lower T_g event is close to that of amorphous felodipine (Fig. 9). It is difficult to infer much information about the composition of the polymer rich phase from the DSC results since it is suspected that remixing is occurring during the DSC scan; hence a clear increase in T_g is observed when cycling the sample through increasingly high temperatures (Fig. 10) and the single T_g event on the second scan (Fig. 9). However, microscopic evidence suggests that the discontinuous phase forms islands of about 300–500 nm diameter (Figs. 13 and 14d).

In considering the mechanism of phase separation, it is probable that the moisture induced immiscibility arises from the altered thermodynamics of the system since the two components appear to be miscible in the absence of water based on the DSC and IR results. Furthermore, the Flory Huggins interaction parameter (χ) between felodipine and PVP (χ_{23}) has been estimated to be slightly negative,⁴³ indicating favorable interactions and confirming the miscibility of these two components. The supposition that the moisture induced phase separation observed in this study has a thermodynamic origin is well supported by the polymer literature where it has been observed that phase separation is promoted when there is asymmetry in the interactions of the two components with the solvent,^{39,40} as in our case. This asymmetry is reflected by large differences in the Flory Huggins binary interaction parameters of each component with the solvent and has been termed the $\Delta\chi$ effect (where $|\Delta\chi| = |\chi_{12} - \chi_{13}|$).^{39,40} The interaction parameters for water and PVP (χ_{13}) and water and felodipine (χ_{12}) are around 0.5⁴⁴ and 3.3⁴⁵ respectively. The large positive interaction parameter for felodipine indicates extremely unfavorable interactions with water, as expected for a hydrophobic drug. The much

smaller value of the interaction parameter for PVP reflects its more hydrophilic nature. There is clearly a large $\Delta\chi$ for this system and indeed a decrease of mixing is observed when either the solid dispersions are exposed to moisture or prepared with water added to the solvent. Bhattacharyya et al.⁴⁶ reported a particularly interesting study where small amounts of moisture present in the organic solvent used to prepare a polymer blend resulted in phase separation. Analogous phenomena have reported for numerous binary polymer systems whereby a certain solvent induces immiscibility in polymer blends known to be compatible.^{47–51} However, water most likely has a dual role in facilitating phase separation, since the absorbed moisture will also increase molecular mobility, allowing the molecules to diffuse to form drug-rich and polymer-rich regions. When water is removed, the system can potentially remix since a thermodynamic driving force exists (because the binary system is miscible and therefore at a lower free energy than the two phase system), however it appears that the kinetics of mixing at room temperature is prohibitively slow, and the decreased drug-polymer interactions persist after the water is removed. For example, Figures 4, 5, and 7 show that water interrupts drug polymer bonds and that these bonds do not reform upon water removal even though the two phases are in close contact with each other. This is presumably related to the fact that each meta-stable phase is in the glassy regime (a reasonable assumption since the T_g of felodipine is around 46°C and the T_g of PVP is about 150°C).^{20,21} Thus two metastable phases are able to persist at room temperature when the moisture is removed. Similar results have been observed for polymer blends cast from solvents. When the temperature is raised to 125°C, which is well above the T_g of felodipine (and that of the corresponding one phase dispersion which is about 80°C), remixing occurs over a period of several hours (Fig. 11) and the remixing at higher temperature supports the supposition that amorphous felodipine and PVP are miscible in the absence of moisture.

The observation that moisture can induce immiscibility is important for several aspects of pharmaceutical development. First, it is clear that the water content of solvents used during the processing operation should be controlled since the solvent composition can dictate if the system is rendered miscible or immiscible. Second, exposure to high relative humidity may influence the

crystallization tendency by altering the number of meta-stable phases. If water sorption leads to phase separation, then the stabilizing influence of the polymer will be reduced in the drug rich phase and the crystallization kinetics are likely to be very different than for a miscible system. Thus, the introduction of a third component (in this case water) may compromise the “stability” of the meta-stable amorphous dispersion and impact the kinetics and thermodynamics of crystallization. Clearly more work is needed to understand which drug–polymer combinations are susceptible to moisture-induced immiscibility. In addition, given the experimental difficulties associated with establishing miscibility, more effort needs to be directed towards determining which analytical techniques are most suitable to probe this phenomenon.

CONCLUSIONS

The strength and extent of hydrogen bonding interactions in felodipine-PVP amorphous dispersions were shown to vary with (i) temperature and (ii) the presence of sorbed water. On increasing the temperature, hydrogen bonding interactions were found to weaken as expected. The effect of temperature on the molecular structure of the amorphous dispersions was found to be reversible. The presence of sorbed water was found to have a much more drastic effect on the amorphous dispersions. Specifically, drug–polymer interactions were lost and drug–drug interactions were formed when water was introduced to the system indicating that moisture induced amorphous–amorphous phase separation. DSC, AFM, and TEM results provided supplementary evidence for the moisture induced immiscibility. Remixing did not occur at room temperature following removal of moisture, but did take place following heating to 125°C. Thus the moisture induced immiscibility is effectively irreversible at low temperature due to the hindered kinetics of the system and may compromise the integrity of the dispersion.

ACKNOWLEDGMENTS

Purdue Life Science Microscopy Facility (LSMF) is acknowledged for the use of their TEM instrument and Ravi Sinha is thanked for assistance with running samples. Jessica Brown and Lindsay Stanford are acknowledged their help

in collecting the FTIR data. Bonnie Co from Purdue University Department of Food Science and Debra Sherman from Purdue LSMF are thanked for their help in conducting AFM and TEM experiments. Leon Farber is acknowledged for his helpful discussions around microscopy techniques. This work was supported in part by a fellowship from Merck Research Laboratories. AstraZeneca and the Dane O. Kildsig Center Pharmaceutical Processing Research are acknowledged for financial support.

REFERENCES

1. Miyazaki T, Yoshioka S, Aso Y, Kojima S. 2004. Ability of polyvinylpyrrolidone and polyacrylic acid to inhibit the crystallization of amorphous acetaminophen. *J Pharm Sci* 93:2710–2717.
2. Seow CC, Cheah PB, Chang YP. 1999. Antiplastization by water in reduced-moisture food systems. *J Food Sci* 64:576–581.
3. Hancock BC, Zografi G. 1994. The relationship between the glass-transition temperature and the water-content of amorphous pharmaceutical solids. *Pharm Res* 11:471–477.
4. Zhang J, Zografi G. 2001. Water vapor absorption into amorphous sucrose-poly(vinyl pyrrolidone) and trehalose-poly(vinyl pyrrolidone) mixtures. *J Pharm Sci* 90:1375–1385.
5. Marsac PJ, Konno H, Rumondor A, Taylor LS. 2008. Recrystallization of nifedipine and felodipine from amorphous molecular level solid dispersions containing poly(vinylpyrrolidone) and sorbed water. *Pharm Res* 25:647–656.
6. Schmitt E, Davis CW, Long ST. 1996. Moisture-dependent crystallization of amorphous lamotrigine mesylate. *J Pharm Sci* 85:1215–1219.
7. Andronis V, Yoshioka M, Zografi G. 1997. Effects of sorbed water on the crystallization of indomethacin from the amorphous state. *J Pharm Sci* 86:346–351.
8. Aso Y, Yoshioka S, Kojima S. 2004. Molecular mobility-based estimation of the crystallization rates of amorphous nifedipine and phenobarbital in poly-(vinylpyrrolidone) solid dispersions. *J Pharm Sci* 93:384–391.
9. Wexler A, Hasegawa S. 1954. Relative humidity-temperature relationships of some saturated salt solutions in the temperature range 0-Degree to 50-Degrees-C. *J Res Natl Bureau Stand* 53:19–26.
10. Konno H, Taylor LS. 2006. Influence of different polymers on the crystallization tendency of molecularly dispersed amorphous felodipine. *J Pharm Sci* 95:2692–2705.
11. Tang XLC, Pikal MJ, Taylor LS. 2002. The effect of temperature on hydrogen bonding in crystalline and amorphous phases in dihydropyridine calcium channel blockers. *Pharm Res* 19:484–490.

12. Coleman MM, Graf JF, Painter PC. 1991. Specific interactions and the miscibility of polymer blends. Lancaster, Pennsylvania: Technomic Publishing AG.
13. Painter PC, Graf JF, Coleman MM. 1991. Effect of hydrogen-bonding on the enthalpy of mixing and the composition dependence of the glass-transition temperature in polymer blends. *Macromolecules* 24:5630–5638.
14. Skrovanek DJ, Howe SE, Painter PC, Coleman MM. 1985. Hydrogen-bonding in polymers—Infrared temperature studies of an amorphous polyamide. *Macromolecules* 18:1676–1683.
15. Coleman MM, Painter PC. 1995. Hydrogen-bonded polymer blends. *Prog Polym Sci* 20:1–59.
16. Park Y, Veytsman B, Coleman M, Painter P. 2005. The miscibility of hydrogen-bonded polymer blends: Two self-associating polymers. *Macromolecules* 38:3703–3707.
17. Desseyn HO, Clou K, Keuleers R, Miao R, Van Doren VE, Bleton N. 2001. The effect of pressure and temperature on the vibrational spectra of different hydrogen bonded systems. *Spectrochim Acta A Mol Biomol Spectrosc* 57:231–246.
18. Kerc J, Srcic S, Mohar M, Smidkorbar J. 1991. Some physicochemical properties of glassy felodipine. *Int J Pharm* 68:25–33.
19. Marsac PJ, Konno H, Taylor LS. 2006. A comparison of the physical stability of amorphous felodipine and nifedipine systems. *Pharm Res* 23:2306–2316.
20. Matsumoto T, Zografi G. 1999. Physical properties of solid molecular dispersions of indomethacin with poly(vinylpyrrolidone) and poly(vinylpyrrolidone-co-vinylacetate) in relation to indomethacin crystallization. *Pharm Res* 16:1722–1728.
21. Zhang J, Zografi G. 2000. The relationship between “BET”- and “Free volume”-derived parameters for water vapor absorption into amorphous solids. *J Pharm Sci* 89:1063–1072.
22. Turnbull D, Fisher JC. 1949. Rate of nucleation in condensed systems. *J Chem Phys* 17:71–73.
23. Fisher JC, Hollomon JH, Turnbull D. 1949. Rate of nucleation of solid particles in a subcooled liquid. *Science* 109:168–169.
24. Fisher JC, Hollomon JH, Turnbull D. 1948. Nucleation. *J Appl Phys* 19:775–784.
25. Marsac PJ, Shamblin SL, Taylor LS. 2006. Theoretical and practical approaches for prediction of drug-polymer miscibility and solubility. *Pharm Res* 23:2417–2426.
26. Sandler SI. 1999. *Chemical & engineering thermodynamics*. 3rd edition. New York: John Wiley & Sons, Inc.
27. Crowley KJ, Zografi G. 2003. The effect of low concentrations of molecularly dispersed poly(vinylpyrrolidone) on indomethacin crystallization from the amorphous state. *Pharm Res* 20:1417–1422.
28. Stein RS. 1994. Crystallization from polymer blends. *Mater Res Soc Symp Proc* 321:531–542.
29. Taylor LS, Zografi G. 1998. Sugar-polymer hydrogen bond interactions in lyophilized amorphous mixtures. *J Pharm Sci* 87:1615–1621.
30. Taylor LS, Zografi G. 1997. Spectroscopic characterization of interactions between PVP and indomethacin in amorphous molecular dispersions. *Pharm Res* 14:1691–1698.
31. Vasanthavada M, Tong WQ, Joshi Y, Kislalioglu MS. 2005. Phase behavior of amorphous molecular dispersions—II: Role of hydrogen bonding in solid solubility and phase separation kinetics. *Pharm Res* 22:440–448.
32. Martin A. 1993. *Physical pharmacy*. 4th edition. Philadelphia: Lippincott Williams & Wilkins.
33. Young RJ, Lovell PA. 1991. *Introduction to polymers*. 2nd edition. Cheltenham, United Kingdom: Nelson Thornes Ltd.
34. Yalkowsky SH. 1999. *Solubility and solubilization in aqueous media*. New York: Oxford University Press.
35. Tang XLC, Pikal MJ, Taylor LS. 2002. A spectroscopic investigation of hydrogen bond patterns in crystalline and amorphous phases in dihydropyridine calcium channel blockers. *Pharm Res* 19:477–483.
36. Lu Q, Zografi G. 1998. Phase behavior of binary and ternary amorphous mixtures containing indomethacin, citric acid, and PVP. *Pharm Res* 15:1202–1206.
37. Kelts LW, Landry CJT, Teegarden DM. 1993. 2-dimensional NMR of synthetic-polymers—Polymer blend miscibility at the molecular-level. *Macromolecules* 26:2941–2949.
38. Bank M, Leffingw J, Thies C. 1971. Influence of solvent upon compatibility of polystyrene and poly(vinyl methyl ether). *Macromolecules* 4:43–&.
39. Pouchly J, Patterson D. 1976. Polymers in mixed solvents. *Macromolecules* 9:574–579.
40. Robard A, Patterson D, Delmas G. 1977. Delta-chi effect and polystyrene poly(vinyl methyl-ether) compatibility in solution. *Macromolecules* 10:706–708.
41. Gregorowicz J, Luszczuk M. 2007. Impact of water on the miscibility of DAB-dendr-(NH₂)(64) and benzene. *Macromolecules* 40:5966–5972.
42. Vasanthavada M, Tong WQ, Joshi Y, Kislalioglu MS. 2004. Phase behavior of amorphous molecular dispersions I: Determination of the degree and mechanism of solid solubility. *Pharm Res* 21:1598–1606.
43. Marsac PJ, Li T, Taylor LS. 2009. Estimation of drug-polymer miscibility and solubility in amorphous solid dispersions using experimentally determined interaction parameters. *Pharm Res* 26:139–151.

44. Hancock BC, Zografi G. 1993. The use of solution theories for predicting water-vapor absorption by amorphous pharmaceutical solids—A test of the Flory-Huggins and Vrentas models. *Pharm Res* 10:1262–1267.
45. χ parameter between the drug, water was obtained using Flory Huggins theory as described in ref 44, fitting moisture sorption data presented in Marsac PJ, Konno H, Rumondor ACF, Taylor LS, 2008. Recrystallization of nifedipine and felodipine from amorphous molecular level solid dispersions containing poly(vinylpyrrolidone) and sorbed water. *Pharm Res* 25:647–656.
46. Bhattacharyya C, Maiti N, Mandal BM, Bhattacharyya SN. 1989. Sensitivity of ternary phase-diagrams of miscible polymer pairs in common solvents to traces of water—Solvent poly(ethyl acrylate) poly(vinyl propionate) and solvent poly(methyl acrylate) poly(vinyl acetate) systems. *Macromolecules* 22:487–489.
47. Landry MR, Massa DJ, Landry CJT, Teegarden DM, Colby RH, Long TE, Henrichs PM. 1994. A survey of polyvinylphenol blend miscibility. *J Appl Polym Sci* 54:991–1011.
48. Ha CS, Lee WK, Cho WJ. *Polymex-93: International Symposium on Polymers, Cancun, Mexico, Nov 01–05 1993*, p. 279–288.
49. Einaga Y. 1994. Thermodynamics of polymer-solutions and mixtures. *Prog Polym Sci* 19:1–28.
50. Hellmann EH, Hellmann GP, Rennie AR. 1991. Solvent-induced phase-separation in polycarbonate blends pc/tmpc. *Colloid Polym Sci* 269:343–352.
51. Saeki S, Cowie JMG, McEwen IJ. 1983. The effect of molecular-weight and casting solvent on the miscibility of polystyrene poly(alpha-methyl styrene) blends. *Polymer* 24:60–64.